

# ONLINE ESTIMATION OF WIND TURBINE BLADE DEFLECTION WITH UWB SIGNALS

Tobias Lindstrøm Jensen<sup>1</sup>, Morten Lomholt Jakobsen<sup>1</sup>, Jan Østergaard<sup>1</sup>, Jesper Kjær Nielsen<sup>1,3</sup>,  
Claus Byskov<sup>2</sup>, Peter Bæk<sup>2</sup> and Søren Holdt Jensen<sup>1</sup>

<sup>1</sup>Department of Electronic Systems, Aalborg University, Denmark

<sup>2</sup>LM Wind Power, Kolding, Denmark

<sup>3</sup>Bang & Olufsen A/S, Struer, Denmark

## ABSTRACT

In this paper we use ultra-wideband (UWB) signals for the localization of blade tips on wind turbines. Our approach is to acquire two separate distances to each tip via time-delay estimation, and each tip is then localized by triangulation. We derive an approximate maximum a posteriori (MAP) delay estimator exploiting i) contextual prior information and ii) a direct-path approximation. The resulting deflection estimation algorithm is computationally feasible for online usage. Simulation studies are conducted to assess the overall triangulation uncertainty and it is observed that negative correlation between the two distance estimates is detrimental for the tip localization accuracy. Measurement data acquired in an anechoic chamber is used to confirm that the UWB-hardware complies with the desired/relevant ranging accuracy. Finally, measurement data obtained from a static test bench is used to demonstrate that the approximate MAP-based localization algorithm is able to outperform standard methods.

**Index Terms**— Wind turbines, blade deflection, localization, UWB signals, time-delay estimation, MAP estimation.

## 1. INTRODUCTION

A key measure in energy production is the levelized cost of energy (LCoE), a per MWh inflation adjusted project-specific cost of producing electricity (assuming a 10% rate of return [1] under current market conditions). To increase market penetration for renewable energy sources, it is necessary to be competitive on key metrics such as LCoE. Wind turbines blade length have increased since the invention of the modern wind turbine in order to increase the amount of energy that can be harvested from the wind. Since the power that can be harvested is proportional to the encircled area (blade length squared), even a modest increase in the blade length has a substantial impact on the amount of energy a wind turbine can produce, cf. [2]. However, a longer blade requires an increase in the blade mass to have a stiffness that will limit

blade deflection in the wind to ensure historically defined safety margins for tower clearance. An increased blade mass also turns into increased production and installation cost. However, blades are currently designed in a conservative manner to ensure safety margins and no methods, like [3], measures the deflection in operation. If the blade deflection can be reliably estimated during operation it opens up new possibilities with respect to design, safety, etc., and may allow for longer blades without the same need for an increase of mass/stiffness. The potential outcome is reduced LCoE and hence an increased market penetration of renewable energy from wind turbines. This paper proposes a wing tip localization design based on ultra-wide band (UWB) hardware and we focus on estimating the blade deflection within accuracies of practical relevance.

UWB time-delay estimation is a known and well-proven technology for position and range estimation, see e.g. the overview work [4,5]. Threshold-based delay estimators [6–8] are sufficiently simple and suitable for low power systems, but the accuracy is governed by the sampling period. One important aspect is to have an algorithm that can provide “accurate-enough” time of arrival estimates under complexity and latency constraints. Estimation tasks in multi-path environments are challenging and often formulated as maximum likelihood (ML) problems which are computationally demanding in general. Approximations such as the WRE-LAX [9] algorithm tries to solve the ML problem iteratively under a zero-mean white Gaussian noise assumption. Other ML approximations or ML-inspired algorithms are [10, 11].

A shortcoming of ML-based estimators is that geometric/physical knowledge about the wind turbine blade is not taken into account. A blade cannot bend arbitrarily in the wind and this (a priori) fact constrains the tip deflection and the time-delay interval in which the direct path can be located (when UWB antennas are mounted at each of the end points of the blade [12]). This motivates the use of a Bayesian approach for tip deflection estimation since the contextual a priori knowledge can be taken directly into account. We employ a maximum a posteriori (MAP) strategy and make a first-incoming signal path approximation suitable for the application at hand. The proposed MAP-based algorithm is only slightly more computational demanding than the correlation

This work was supported by the The Danish National Advanced Technology Foundation with project title “Intelligent rotor for wind energy cost reduction”. The work of T.L. Jensen was partly supported by the Independent Research Council for Technology and Production 4005-00122. The work of J.K. Nielsen is supported by the Danish “InnovationsFonden”.

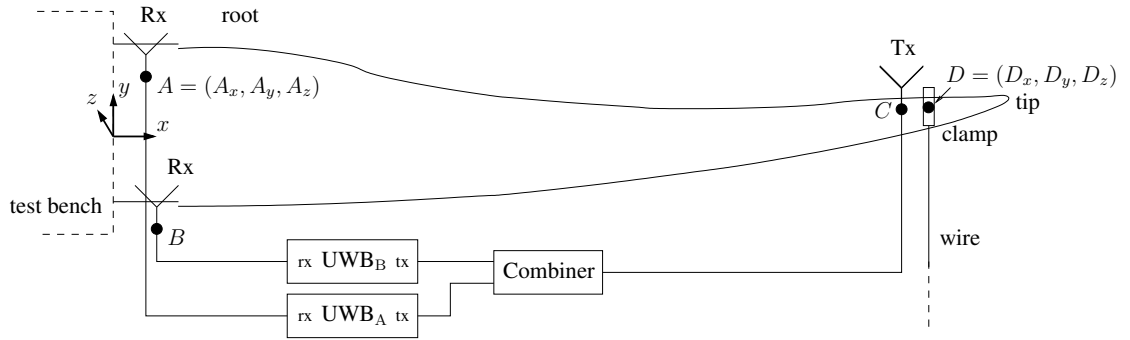


**Fig. 1.** Measurement setup using a static test bench. Top view. The deflection is defined as  $d = -D_y$ . Using a clamp and a wire it is possible to have deflections  $d \in [-1.0, 1.45]$  since the blade has a pre-bend of 1.0 [m] in the positive  $y$ -direction.

method [13], making it suitable for online processing.

The main contributions of this paper consist of an application-tailored approximate MAP time-delay estimator, our simulation study (assessing triangulation uncertainty as a function of ranging uncertainties) and our results from processing of real measurement data (anechoic chamber and static test bench) acquired specifically to answer questions related to the practical feasibility of the proposed signal processing algorithm and UWB-design.

## 2. TEST BENCH MEASUREMENT SETUP

For illustration of the conceptual idea, Fig. 1 shows a controlled measurement setup with a 37.3 [m] wind turbine blade mounted at a static test bench. Three UWB-antennas are installed on the blade: one interior Tx placed underneath the leading edge surface at the tip end, and two exterior Rx placed  $\simeq 0.4$  [m] above the blade surface at the root end (about 2.35 [m] from each other). The interior Tx a directional and vivaldi type antenna with a small and stable gain center [14] whereas the exterior Rx antennas are regular horn antennas. The antennas are connected to two UWB-radios and a combiner. The radios are denoted by  $UWB_A$  and  $UWB_B$  and they both operate with a sampling period of  $T_s = 61 \cdot 10^{-12}$  [s] in the frequency band from 3.1 to 5.3 [GHz] with a center frequency of  $f_c = 4.3 \cdot 10^9$  [Hz]. The two radios are controlled to support time-division multiplexing and transmit a known template signal (see Fig. 5 (a) in Sec. 6) from the Tx antenna at point  $C$  to the Rx antennas at point  $A, B$  of which only one is received by either  $UWB_A$  and  $UWB_B$ . The distance  $d_{AC} = \|A - C\|_2$  from point  $A$  to  $C$  may be estimated via the standard Time-of-Arrival (ToA) method

$$\hat{d}_{AC} = (\hat{\tau} - o_{AC})c_{\text{air}} \quad (1)$$

where  $\hat{\tau}$  is the estimated round trip delay,  $o_{AC}$  is the (offset/constant) time-delay in wires, combiner, etc., and  $c_{\text{air}}$  is the speed of light in atmospheric air. The blade deflection on Fig. 1 is defined as  $d = -D_y$  and can be altered using a clamp and a wire. Since the Tx is at point  $C$  and not  $D$ , the estimated deflection at the clamp is calculated using  $\hat{d} = -C_y\beta$ , where

$\beta = 1.089$  is suggested by a blade model. Due to the geometry and the physical extent of a 37.3 [m] blade, the ranges  $d_{AC}, d_{BC}$  can vary in the order of  $\simeq 0.5$  m. In the following we describe how the round trip delay estimate  $\hat{\tau}$  is acquired.

## 3. SIGNAL MODEL AND TIME-DELAY ESTIMATOR

A natural choice is to consider the sampled multi-path model

$$y(nT_s) = \sum_{\ell=1}^L \alpha_{\ell} x(nT_s - \tau_{\ell}) + e(nT_s), \quad n = 0, \dots, N \quad (2)$$

where  $y(t)$  denotes the received signal composed of  $L$  individually delayed and scaled replicas of the known transmit/template signal  $x(t)$  embedded in noise  $e(t)$ . The parameters of the model in (2) are the integer  $L$ , amplitudes  $\{\alpha_{\ell}\}$ , and delays  $\{\tau_{\ell}\}$  which are conveniently ordered with  $\tau_1 < \tau_2 < \dots < \tau_L$ . For range estimation purposes the main interest usually lies with the earliest delay  $\tau_1$  (direct path) and all other parameters are of nuisance or auxiliary type. Now, if the two earliest signal replicas/multi-path components are (at least partly) separable in delay, meaning that  $\tau_2 - \tau_1 \geq \Delta$ , then by restricting the number of samples we have

$$y(nT_s) = \alpha_1 x(nT_s - \tau_1) + e(nT_s), \quad n = 0, \dots, \tilde{N}(\tau_1) \quad (3)$$

where  $\tilde{N}(\tau_1) < N$ . Both  $\Delta$  and  $\tilde{N}(\tau_1)$  depends on the effective duration of the template signal  $x(t)$  and for the model in (3) to be sensible we should have  $\tilde{N}(\tau_1)T_s \leq \tau_2$  (coarsely verified by inspection of received training signals). We proceed by invoking a set of assumptions on the model in (3):

- The noise is such that  $e(t) \sim \mathcal{N}(0, \sigma_e^2)$  and  $E[e(t)e(t - \kappa)] = 0, \kappa \neq 0$ , i.e.  $e(t)$  is a white Gaussian process.
- A priori the parameters  $\tau_1$  and  $\alpha_1$  are independent, i.e.  $p(\tau_1, \alpha_1) = p(\tau_1)p(\alpha_1)$ .
- The direct path carries a specific “least-amount” of energy and does not contain a  $-180^\circ$  phase shift. This simplifying assumption supports a threshold-type (improper) prior  $p(\alpha_1) \propto I_{\mathcal{A}}(\alpha)$ ,  $\mathcal{A} = \{\alpha \mid \alpha \geq \alpha_{1\text{east}}\}$  where  $I_{\mathcal{A}}$  is the indicator function of the set  $\mathcal{A}$  and where  $\alpha_{1\text{east}} > 0$  is a tunable design-parameter.

- For simplicity, the direct path delay is assumed to follow a uniform distribution such that  $\tau_1 \sim \mathcal{U}(D_L, D_U)$  with (Lower and Upper) boundaries determined by the physical extent of the wind turbine blade.

Our a priori assumptions on  $\tau_1$  and  $\alpha_1$  are targeting simplicity to give rise to a MAP-based estimator with the ability to both “mimic” and improve the classical correlation method [13]. Assume for the moment that  $\tilde{N}(\tau_1) = \tilde{N}$  is constant. Then the MAP-estimate of  $(\tau_1, \alpha_1)$  given  $\{y(nT_s)\}_{n=0}^{\tilde{N}}$  reads

$$\hat{\tau}_1, \hat{\alpha}_1 = \underset{\tau_1, \alpha_1}{\operatorname{argmax}} p\left(\tau_1, \alpha_1 \mid \{y(nT_s)\}_{n=0}^{\tilde{N}}\right) \quad (4)$$

$$= \underset{\substack{\alpha_1 \geq \alpha_{1\text{least}} \\ D_L \leq \tau_1 \leq D_U}}{\operatorname{argmin}} \sum_{n=0}^{\tilde{N}} \left(y(nT_s) - \alpha_1 x(nT_s - \tau_1)\right)^2. \quad (5)$$

Notice that for any fixed choice of  $\tau_1$ , the “remaining” minimization task in (5) is a convex constrained least-squares problem in  $\alpha_1$ . With this in mind we now wish to conveniently avoid the formal delay-dependency on  $\tilde{N}(\tau_1)$  and also to get to work with vectors (of constant length). Accordingly, we define a delay-dependent moving window of  $W$  samples with (Lower and Upper) boundaries selected such that  $W = W_U(\tau_1) - W_L(\tau_1) + 1$  and such that  $T_s W_U(D_U) - D_U \leq \Delta$ , i.e. we do not delay our template signal  $x(t)$  “out-of-bounds”. With simplified notation  $\tau = \tau_1$  and  $\alpha = \alpha_1$  we then approximate the minimization task in (5) by

$$\min_{D_L \leq \tau \leq D_U} \min_{\alpha \geq \alpha_{1\text{least}}} \sum_{n=W_L(\tau)}^{W_U(\tau)} \left(y(nT_s) - \alpha \bar{x}(nT_s - \tau)\right)^2 \quad (6)$$

where  $\bar{x}(t) = x(t)I_{[0, \Delta]}(t)$  denotes an appropriately truncated version of the original template signal  $x(t)$ . For fixed  $\tau$ , the inner minimization task in (6) remains a convex constrained least-squares problem and this fact allow us to state that an approximate MAP estimate of  $\tau = \tau_1$  reads

$$\hat{\tau} = \theta(\{y(nT_s)\}_{n=0}^{\tilde{N}}) = \underset{D_L \leq \tau \leq D_U}{\operatorname{argmin}} \|y_\tau - \alpha_\tau^* \bar{x}_\tau\|_2^2, \quad (7)$$

where in (7) we have solved the inner minimization problem from (6). The solution is delay-dependent and given by

$$\alpha_\tau^* = \max\left(\alpha_{1\text{least}}, \frac{\bar{x}_\tau^T y_\tau}{\|\bar{x}_\tau\|_2^2}\right) \quad (8)$$

and where we also introduced the two delay-dependent constant-length vectors

$$\bar{x}_\tau = [\bar{x}(W_L(\tau)T_s - \tau), \dots, \bar{x}(W_U(\tau)T_s - \tau)]^T \quad (9)$$

$$y_\tau = [y(W_L(\tau)T_s), \dots, y(W_U(\tau)T_s)]^T. \quad (10)$$

To relate the estimator in (7) with a classical time-delay estimation method, we emphasize that the quantity  $\bar{x}_\tau^T y_\tau$  in (8) is the output of the correlation method [13] using the template

$\bar{x}_\tau$  and delay  $\tau$  (and when the threshold-parameter  $\alpha_{1\text{least}}$  is chosen sufficiently large, the estimator in (7) effectively acts like the correlation method). The minimization problem in (7) is one-dimensional in  $\tau$  and can be approximately solved by the grid method in the interval  $\tau \in [D_L, D_U]$ . We choose this method due to an oscillating behavior of the objective function  $\|y_\tau - \alpha_\tau^* \bar{x}_\tau\|_2^2$  originating in part from the shape of the template signal  $x(t)$ , see also [15]. For simplicity, let  $D_L, D_U$  be on the sampling grid. Then test  $\tau \in \{D_L + vk \mid k = 0, \dots, Z\}$ ,  $v = (D_U - D_L)/Z$  i.e.  $Z+1$  evenly spaced points. We select  $Z = K(D_U - D_L)/T_s$ , i.e.  $v = \frac{T_s}{K}$  or  $K$ -fold over-sampling. The algorithm then has the time-complexity  $\mathcal{O}(WK \frac{D_U - D_L}{T_s})$  and requires about three times as many operations as the  $K$ -fold over-sampled correlation method. A variation is to first select a coarse grid, and then perform line-search around the coarse minimum [15]. To be able to evaluate (8)–(9), an approximate continuous representation  $x(t)$  was found via cubic interpolation of the sampled signal to be used for an odd-numbered  $K$ -fold over-sampling (by phase-shifting) as opposed to the use of a single over-sampled template. Thus, we create a bank of  $K$  template signals where  $(K-1)/2$  are slightly anticipated and  $(K-1)/2$  are slightly delayed. Note that this is possible to precompute offline.

#### 4. TRIANGULATION ACCURACY

From the time-delay estimator (7) and the ToA-model (1) we obtain estimates  $\hat{d}_{AC}, \hat{d}_{BC}$  which are used to estimate the blade deflection via triangulation. A standing assumption is that the stiffness of the blade along the flap-wise direction makes the blade movement restricted to a single plane. In this case it is sufficient with two distances to estimate coordinate  $C$  and hence the deflection  $d$ , recall Fig. 1.

Since the two reference points  $A$  and  $B$  in the triangulation are close, the deflection estimate is expected to be sensitive to the accuracy of the range estimates  $\hat{d}_{AC}$  and  $\hat{d}_{BC}$ . To assess this we conduct a simplifying Monte Carlo study in which we draw a random deflection  $d \sim \mathcal{U}(-1.2, 4.8)$ , a reasonable deflection range for a 37.3 [m] blade, and calculate the “true” ranges  $d_{AC}$  and  $d_{BC}$  corresponding to the simulated outcome of  $d$  (for convenience we use a fixed  $x$ -coordinate of the point  $C$ ). We then invoke the simplistic range error model:

$$\begin{bmatrix} \hat{d}_{AC} \\ \hat{d}_{BC} \end{bmatrix} = \begin{bmatrix} d_{AC} \\ d_{BC} \end{bmatrix} + \begin{bmatrix} w_{AC} \\ w_{BC} \end{bmatrix} \quad (11)$$

where the two range errors have a joint distribution

$$\begin{bmatrix} w_{AC} \\ w_{BC} \end{bmatrix} \sim \mathcal{N}\left(\begin{bmatrix} 0 \\ 0 \end{bmatrix}, \sigma_w^2 \begin{bmatrix} 1 & \rho \\ \rho & 1 \end{bmatrix}\right). \quad (12)$$

The goal is to evaluate the standard deviation of the deflection error  $d_e = d - \hat{d} = T(d_{AC}, d_{BC}) - T(\hat{d}_{AC}, \hat{d}_{BC})$ , where  $T$  is the triangulation function. We monitor the behavior of  $\operatorname{std}(d_e)$  as a function of the two parameters in (12), namely

the spread  $\sigma_w$  and the correlation coefficient  $\rho$  (non-zero e.g. if the ToA model (1) is incorrect at certain deflections). Fig. 2 shows the result of 50000 Monte Carlo repetitions. In practice we are interested in accuracies such that  $\text{std}(d_e) \simeq 0.1$  [m]. For our 37.3 m blade, the Monte Carlo study suggests (as a guideline) that we need a ranging accuracy in the order of 4 [mm], provided that the range estimates  $\hat{d}_{AC}$  and  $\hat{d}_{BC}$  are uncorrelated. A practically relevant observation (compliant with intuition), is that negative correlation between  $\hat{d}_{AC}$  and  $\hat{d}_{BC}$  is detrimental to triangulation accuracy.

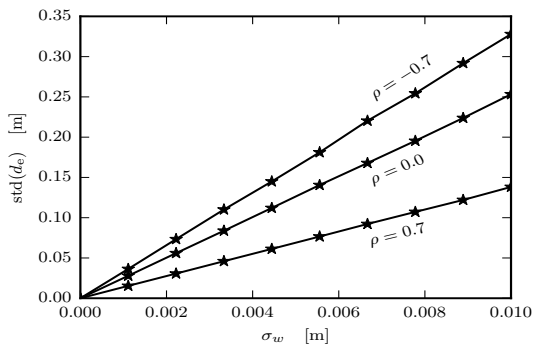


Fig. 2. Average triangulation error as a function of the two range errors' spread  $\sigma_w$  and their correlation  $\rho$ .

## 5. CONTROLLED TESTS IN ANECHOIC CHAMBER

The following two tests were conducted to assess the ranging accuracy to be expected in (1) as a function of UWB-hardware capabilities and the time-delay estimator (7). Thus, our tests do not involve triangulation but merely a single Tx and Rx antenna displaced approximately 4 [m] in an anechoic chamber (guaranteeing  $L = 1$  in (2)). The first test moves Tx in steps of  $d_s = 2.5$  [mm] in total 10 points  $d_{1,v} = vd_s, v = 0, 1, \dots, 9$ . Using the estimator (7) we then obtain  $\hat{d}_{1,v} = (\theta(y_v) - o)c_{\text{air}}$  where the offset  $o$  is selected such that  $\hat{d}_{1,0} - \hat{d}_{1,0} = 0$  (serving as a reference) and  $y_v$  is the received signal under test  $v$ . The results are depicted in Fig. 3 with each curve showing an average of 50 repetitions of the test (but results from all 50 repetitions are consistent).

When the blade is bend, the angle between Tx and Rx antennas changes. The impact of this is assessed in a second test where the Tx antenna is rotated  $\phi$  [degrees $^\circ$ ] around the phase center relative to Rx and the distance  $\hat{d}_{2,\phi}$  is estimated in a similar way as in the first test. However, the offset  $o$  is now selected such that  $\hat{d}_{2,0} = 0$  serves as a reference point. The results are depicted in Fig. 4, showing again an average over 50 repetitions of the test (results again consistent within an error smaller than the resolution  $T_s c_{\text{air}}/K$ , which is approximately 1 and 0.4 [mm] for  $K = 19$  and 49, respectively).

From these two anechoic tests we conclude that the accuracy of the hardware and the estimator (7) is in the order of one millimeter, i.e. within the accuracy put forth in Sec. 4.

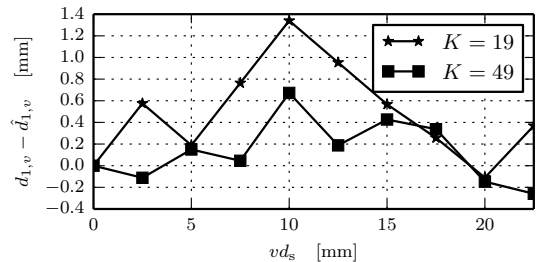


Fig. 3. Tx-Rx displacement in steps of  $d_s = 2.5$  [mm] from a reference point and corresponding estimates using (7). Mean over 50 trials. Over-sampling factor  $K \in \{19, 49\}$ .

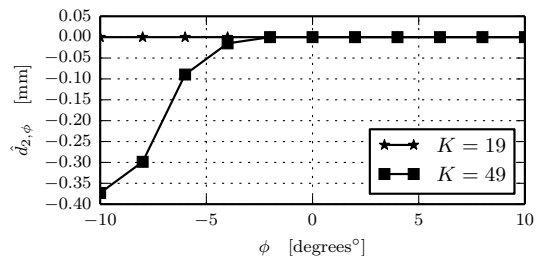


Fig. 4. Tx-rotations  $\phi$  and corresponding estimates using (7). Mean over 50 trials. Over-sampling factor  $K \in \{19, 49\}$ .

## 6. CONTROLLED EXPERIMENT ON TEST BENCH

Finally, the full triangulation-based deflection estimation algorithm is tested on a static test bench as illustrated in Fig. 1. The deflection is measured and controlled using the clamp-and-wire system and serves as “ground-truth” for comparison. A sampled version of the template signal  $x(nT_s)$  for both  $\text{UWB}_A$  and  $\text{UWB}_B$  was acquired via back-to-back measurements (without antennas). The design parameter  $\Delta$  for each channel  $\Delta_{AC}, \Delta_{BC}$  was found by experiment and selected as approximately half of the 0.95 power pulse width. The offsets  $o_{AC}$  and  $o_{BC}$  in (1) was found from a separate experiment with an exterior Tx antenna at the tip. A sequence of pairs of received signals ( $\text{UWB}_A + \text{UWB}_B$ ) were collected while the blade performed a controlled sweep, starting at  $d = 0$  (Straight), then loaded until  $d = 1.45$  and released back to  $d = 0$ . Fig. 5 (a) shows a template signal  $x(nT_s)$  and Fig. 5 (b) shows an example of a received signal  $y(nT_s)$ .

We compare the triangulation performance in three different cases of an underlying ranging (i.e. time-delay) estimator: approximate MAP (proposed,  $K = 19$ ), the correlation method [13], and the WRELAX algorithm [9]. The correlation method has been implemented with a truncated template  $\bar{x}(t) = x(t)I_{[0,\Delta]}(t)$  that yielded the best performance. For the WRELAX algorithm we input  $L$  from (2) as the smallest  $L' \in \{1, \dots, 10\}$  that gives  $\tau_1 \in [D_L, D_U]$ . Deflection estimation results are shown in Fig. 6 together with a curve displaying “ground-truth” deflections for comparison.

The approximate MAP approach seems consistent for all deflections but off by approximately 0.2 [m]. The correla-

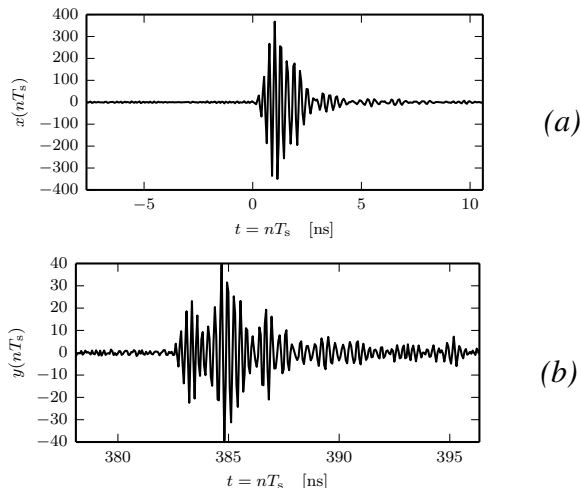


**Fig. 5.** (a) Measured back-to-back template  $x(nT_s)$ . (b) Example of a received signal  $y(nT_s)$  measured at the test bench.

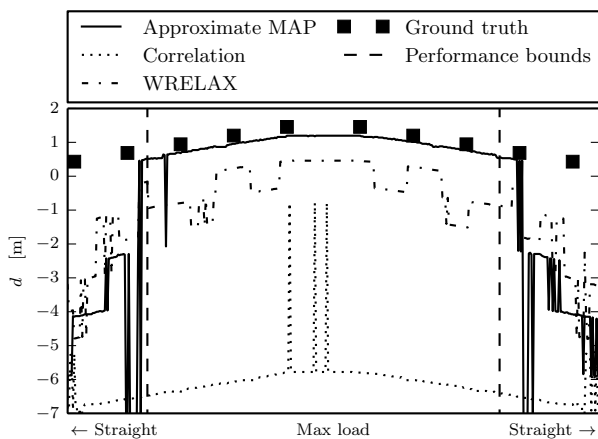


**Fig. 6.** Triangulation-based deflection estimates obtained with different underlying range estimators.

tion method is consistent but way off because it locks onto a strong but delayed signal reflection, see Fig. 5(b). The WRELAX estimator jumps in steps of 0.75 m because it often selects the leading edge half a “period” too late (the period of the template pulse), which results in a range error of approx.  $\frac{c_{air}}{2f_c} \approx 0.035$  [m]. Due to the sensitivity of triangulation, this maps to the approximately 0.75 [m] jumps in deflection.

## 7. CONCLUSIONS AND FUTURE WORK

The proposed approximate MAP-based time-delay estimator is able to deliver pairs of range estimates within practically relevant accuracies for the purpose of triangulation-based wind turbine blade deflection estimation. Our simplified Monte Carlo study confirms that negative correlation among the pair of range estimates is detrimental to the performance of the final triangulation step. Two tests performed in an anechoic chamber reveal that the combination of UWB-hardware

and the approximate MAP-based time-delay estimator leads to ranging accuracies in the order of one millimeter. When operated on a static test bench (giving rise to more realistic propagation conditions) the deflection estimation accuracy is consistent but off by a constants of 0.2 [m]. This error is due to incorrect calibration of  $\sigma_{AC}$  and  $\sigma_{BC}$  in (1) and can be adjusted by a mere 1 [cm] modification.

Future work will consist of investigating and exploiting i) temporal motion of a sweeping blade, and ii) more profound a priori knowledge – both aiming at achieving more accurate and reliable tip localization for longer blades ( $> 37.3$  [m]).

## REFERENCES

- [1] “World Energy Perspective: Cost of Energy Technologies,” Tech. Rep., World Energy Council and Bloomberg New Energy Finance, 2013, [www.worldenergy.org](http://www.worldenergy.org).
- [2] D. E. Berg, “Wind energy conversion,” in *Handbook of Energy Efficiency and Renewable Energy*, F. Kreith and D. Y. Goswami, Eds. CRC Press, 2007.
- [3] C. Kildegaard, “Monitoring the operation of a wind energy plant,” 2011, US Patent US7883316 B2.
- [4] S. Gezici, Z. Tian, G. B. Giannakis, H. Hisashi, A. F. Molisch, H. V. Poor, and Z. Sahinoglu, “Localization via ultra-wideband radios: a look at positioning aspects for future sensor networks,” *Signal Processing Magazine, IEEE*, vol. 22, no. 4, pp. 70–84, July 2005.
- [5] S. Gezici and H. V. Poor, “Position estimation via ultra-wide-band signals,” *Proceedings of the IEEE*, vol. 97, no. 2, pp. 386–403, 2009.
- [6] I. Guvenc and Z. Sahinoglu, “Threshold-based TOA estimation for impulse radio UWB systems,” in *2005 IEEE International Conference on Ultra-Wideband*, 2005, pp. 420–425.
- [7] D. Dardari, C.-C. Chong, and M. Z. Win, “Threshold-based time-of-arrival estimators in UWB dense multipath channels,” *IEEE Transactions on Communications*, vol. 56, no. 8, pp. 1366–1378, 2008.
- [8] M. J. Kuhn, J. Turnmire, M. R. Mahfouz, and A. E. Fathy, “Adaptive leading-edge detection in UWB indoor localization,” in *2010 IEEE Radio and Wireless Symposium (RWS)*, 2010, pp. 268–271.
- [9] J. Li and R. Wu, “An efficient algorithm for time delay estimation,” *IEEE Transactions on Signal Processing*, vol. 46, no. 8, pp. 2231–2235, 1998.
- [10] A. D’Andrea V. Lottici and U. Mengali, “Channel estimation for ultra-wideband communications,” *IEEE Journal on Selected Areas in Communications*, vol. 20, no. 9, pp. 1638–1645, 2002.
- [11] C. Falsi, D. Dardari, L. Mucchi, and M. Z. Win, “Time of arrival estimation for UWB localizers in realistic environments,” *EURASIP Journal on Advances in Signal Processing*, vol. 2006, no. 1, pp. 1–13, 2006.
- [12] C. Byskov, P. Bæk, M. Klitgaard, C. Skovby, and L. Fuglsang, “A blade deflection monitoring system,” 2014, WO Patent App. PCT/EP2013/067,009.
- [13] C. Knapp and G. C. Carter, “The generalized correlation method for estimation of time delay,” *IEEE Transactions on Acoustics, Speech and Signal Processing*, vol. 24, no. 4, pp. 320–327, 1976.
- [14] S. Zhang and G. F. Pedersen, “Modified vivaldi antenna with improved gain and phase center stability,” 2015, submitted.
- [15] R. Wu and J. Li, “Time-delay estimation via optimizing highly oscillatory cost functions,” *IEEE Journal of Oceanic Engineering*, vol. 23, no. 3, pp. 235–244, 1998.